PAPER *Special Issue on Technology Challenges for Single Electron Devices*

Photoirradiation Effects in a Single-Electron Tunnel Junction Array

Michiharu TABE†a), *Member*, Yoichi TERAO†, *Nonmember*, Noboru ASAHI††, *Student Member*, *and* Yoshihito AMEMIYA††, *Member*

SUMMARY Area-restricted illumination of light onto a voltage-biased single-electron tunnel junction array is modeled by reduced resistance of junctions, and its effects on current-voltage characteristics, charge distributions and potential profiles are calculated by a Monte Carlo method. The results show that photocurrent nearly proportional to the applied voltage is generated above a threshold voltage determined by Coulomb blockade effect. The photocurrent increases with increasing irradiated area, which is ascribed to reduction in total resistance of the circuit. Under irradiation, a characteristic charge distribution is formed, i.e., negative and positive charge bumps are formed in the nodes at the dark and bright boundaries. The charge bumps serve to screen the electric field formed by the bias voltage and create almost a flat potential in the irradiated area. Furthermore, time-response of the charge distribution to a pulse irradiation is also studied. For high dark resistance, the charge bumps are sustained for a long period working as a memory of light. These results suggest feasibility of single-electron photonic devices such as photodetectors and photomemories.

key words: *SET, photoirradiation, Monte Carlo simulation, photonic devices*

1. Introduction

Up to now, single-electron tunneling (SET) has been extensively studied to develop mesoscopic electronic devices such as SET transistors and memories. Interactions of electron tunneling with photons, namely photon-assisted tunneling [1], [2], is also attractive in SET device application, because SET can be modulated by photon absorption like the role of the gate bias in the SET transistor. So far, a coupling of SET with a microwave has been used to elucidate time correlation of SET events [3]. For a shorter wavelength, a photodetector utilizing a SET transistor was demonstrated [4], but it detected photoinduced charges produced outside of the transistor without direct SET-photon interactions involved.

Recently, Fujiwara et al. have reported [5] that a visible light influences the I-V characteristics in an SET transistor and that the number of electrons in the central node is exactly known in the conductance oscillation with varying gate voltage. In their work, it is strongly suggested that an excited electron produced by the light tunnels to a lead before recombination, leaving a hole in the node, which results a modulation of the macroscopic I-V characteristics. Although the physics of the photon-assisted tunneling in SET is not quite understood, their work [5] encourages us to study applicability of SET to photonic devices. The advantages of the single-electron photonic devices would be their high spatial resolutions and high sensitivities. The highest limit of spatial resolution in a single-electron photodetector is expected to be close to an area of a single node, which is typically less than $(100\ \mathrm{nm})^2$ and can be further reduced. The sensitivity should strongly depend on the overall device structure and the optical absorption coefficient of the node material, although, once only a few electrons are excited, the circuit current would be significantly enhanced.

The purpose of this work is to study, for the first time, photoirradiation effects on I-V characteristics and charge distributions in a one-dimensional voltage-biased tunnel junction array by Monte Carlo SET simulation. The tunnel junction array seems to be more suitable for the photonic devices than the transistors, in a sense that the irradiation areas can be selected with a wide variety. In this work, we focus only on extracting fundamental photoresponse properties in a tunnel junction array, and do not consider material- and structure-dependent photosensitivities, which will be studied in the future.

2. Calculation Model

A one-dimensional voltage-biased SET array used in this work is shown in Fig. 1 (a), where 20 ultrasmall tunnel junctions are connected in series. Light in a continuous or a pulse mode

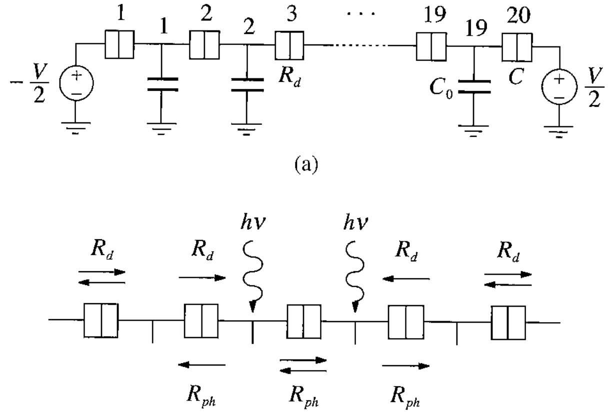

Fig. 1 (a) A voltage-biased one-dimensional tunnel junction array and (b) modeling of area-restricted irradiation of light.

Manuscript received June 5, 1997.
Manuscript revised September 10, 1997.

† The authors are with Research Institute of Electronics, Shizuoka University, Hamamatsu-shi, 432 Japan.
†† The authors are with the Faculty of Engineering, Hokkaido University, Sapporo-shi, 060 Japan.
a) E-mail: romtabe@rie.shizuoka.ac.jp

is locally irradiated onto a number of middle nodes. The nodes and the junctions are numbered from the left to the right, as shown in this figure. The node is assumed to be made of a normal metal or a highly-doped semiconductor with continuous electron energies. Parameter values of the tunnel junction capacitance C, the parasitic capacitance of each node C_0 and the tunnel resistance in the dark R_d are set to be 100 aF, 1 aF and 1 MΩ, respectively.

The irradiation of light is modeled simply by a reduced tunnel resistance R_{ph} (= 100 kΩ < R_d) for the irradiated area, as shown in Fig. 1 (b). This is based on the consideration that, when an electron in one of the irradiated nodes is excited by a photon with an energy of $h\nu$, the effective tunnel barrier for the excited electron to the neighboring node should be lowered by the same energy. The value of 100 kΩ as R_{ph} is chosen for tunneling events to be still dominated by Coulomb blockade even under photoirradiation, because the Coulomb blockade works only when tunnel resistance is higher than the "quantum of resistance," $R_Q = h / 4e^2 \approx 6.5$ kΩ, where h is the Planck constant and e is the elementary charge. In this model, major assumptions are that (i) the number of excited electrons (excitation rate g times recombination lifetime τ) is kept constant in each irradiated node, and (ii) when an excited electron tunnels to the neighboring node, the electron quickly releases the excess energy $h\nu$ and at the same time another electron is instantly excited in the original node before successive tunneling occurs. Therefore, since the energy loss of the tunneling electron is compensated by the excitation of the ground-state electron, the photon energy $h\nu$ does not directly contribute to the free energy of the system. Only the tunnel resistance or tunnel rate is, thus, modulated by photoabsorption; the dark resistance R_d is reduced to a smaller value R_{ph} between irradiated nodes, while at the bright and the dark boundary the tunnel resistance is direction-dependent, i.e., R_{ph} from the bright to the dark node and R_d from the dark to the bright node. Even if these assumptions are partially broken in a practical situation, we believe that the results obtained in this work would not be altered so much, because reduction in tunnel resistance due to irradiation must be always true.

The SET is calculated numerically using a Monte Carlo simulation [6], ignoring co-tunneling effects. Forward and reverse tunneling rates at a junction are give by

$$\Gamma^{\pm}=\frac{1}{e^2R_T}\frac{\Delta E^{\pm}}{\left[1-\exp\left(-\Delta E^{\pm}/k_BT\right)\right]}$$

where R_T is tunnel resistance ($R_T = R_d$ or R_{ph}), and $\Delta E^{\pm}$ is the change in total free energy due to forward and reverse tunneling events including the work done by the voltage source. The temperature T is assumed to be 0 K for simplicity; therefore, $\Gamma^{\pm} = 0$ for $\Delta E^{\pm} < 0$ and $\Gamma^{\pm} = \Delta E^{\pm} / e^2R_T$ for $\Delta E^{\pm} > 0$, indicating that SET is allowed only when the free energy in the whole system is lowered by the tunneling. Because $(\Gamma^{\pm})^{-1}$ is the average interval between successive tunneling events, we calculated tunneling intervals $u^{\pm}$ using a random number r ($0 < r < 1$) by the following equation [6]

$$u^{\pm}=\frac{1}{\Gamma^{\pm}}\ln\left(\frac{1}{r}\right)$$

For all tunnel junctions, we calculate $u^{\pm}$ values and choose a tunneling event with the minimum $u^{\pm}$, which is regarded as tunneling that actually happened. Then we repeat the same procedure starting at $t = u^{\pm}$.

3. Results and Discussion

3.1 Photocurrent

We first simulated current-voltage characteristics of the array under continuous irradiation of light. The results are shown in Fig. 2 (a) in a wide voltage region and (b) in a low voltage region. The dark current is corresponding to Curve A, while the currents under irradiation onto 5 and 11 middle nodes are corresponding to Curve B and Curve C, respectively. Generation of photocurrent, defined as differences from the dark current, is obvious and the photocurrent increases with in-

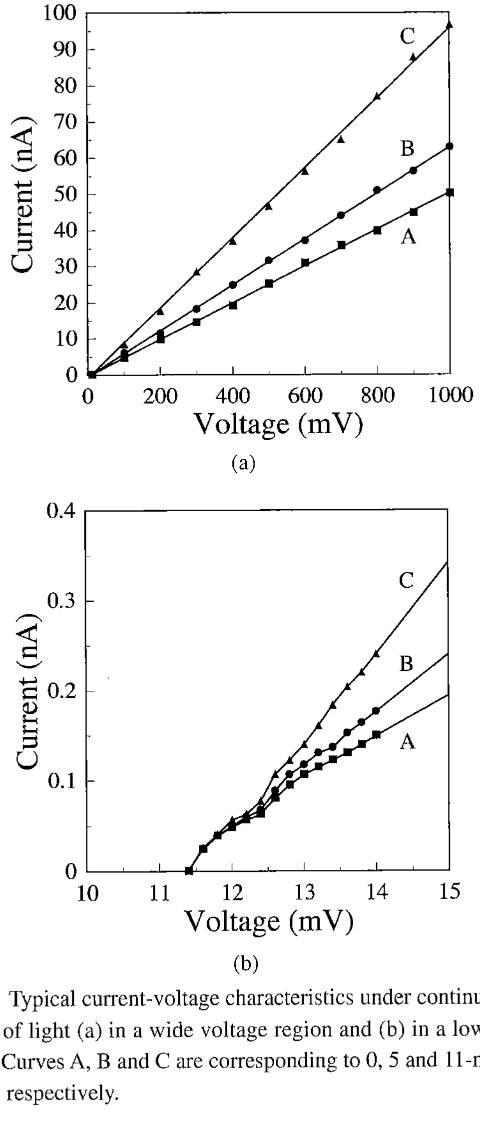

(a)

(b)

Fig. 2 Typical current-voltage characteristics under continuous irradiation of light (a) in a wide voltage region and (b) in a low voltage region. Curves A, B and C are corresponding to 0, 5 and 11-node irradiation, respectively.

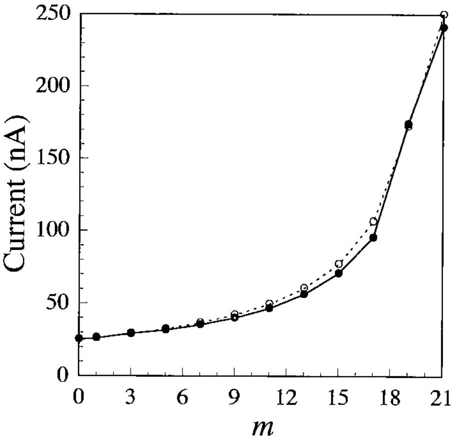

Fig. 3 Circuit current at $V = 500$ mV as a function of the number of irradiated nodes, m. The solid line is a result of Monte Carlo simulation, while the dotted line is obtained from an analytical form (see text).

creasing bias voltage. In Fig. 2 (a), all the curves appear to follow linear voltage dependences, or ohmic dependences, but the non-linear behavior due to the Coulomb blockade is observed in the low voltage region (b). The threshold voltage due to the Coulomb blockade effect remains unchanged (11.4 mV) even under irradiation, because the onset of the current is dominated not by the tunnel resistance but primarily by the values of C and C_0. The non-linear voltage dependence of the dark current (Curve A) in (b) is essentially the same as that reported by Likharev et al. [7].

The circuit current at a relatively high bias voltage, 500 mV, as a function of the number of irradiated nodes is shown by a solid line (and closed circles) in Fig. 3. The current increases gradually and then quickly with increasing irradiation area. The dotted line (and open circles) is an ohmic dependence, ignoring Coulomb blockade effect, expressed by an equation,

$$I = \frac{V}{R_{total}} = \frac{V}{\left[(20 - m)R_d + mR_{ph}\right]},$$

where R_{total} is the total circuit resistance and m is the number of irradiated nodes (the number of junctions with the reduced resistance counted in the direction of the electron flow). Both lines are in good agreement and, therefore, at high bias voltages the overall dependence follows the above equation. It should be noted, however, when the bias voltage is as small as that near the threshold voltage, e.g., below 100 mV, the current significantly deviates from the $1 / R_{total}$ dependence because of the non-linear relationship due to the Coulomb blockade effect.

3.2 Charge Distributions

Charge distributions (number of electrons, n, in each node) in the almost steady state in the array at $V = 500$ mV are shown in Fig. 4, where (a) and (b) are without and with continuous irradiation (5-node irradiation), respectively. In this figure, negative numbers of electrons appear in some nodes, which indicate positive charges resulted from an outflow of electrons. The distribution without irradiation (Fig. 4 (a)) significantly fluctuates in space (and also in time), because the fluctuation is favorably induced in SET process to efficiently dissipate the free energy, as we have previously reported [8]. Time-averaged charges in the dark, however, are close to zero in any node.

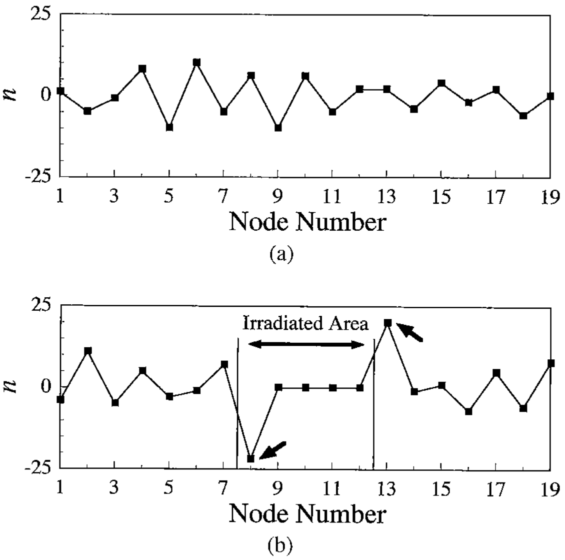

Fig. 4 Charge distributions (number of electrons, n, in each node) at $V = 500$ mV (a) without irradiation and (b) with continuous irradiation onto 5 middle nodes. The arrows in (b) indicate photoinduced charge bumps.

The distribution under irradiation (Fig. 4 (b)) is interesting, because negative and positive bumps are built up at the edges of the irradiated area, as indicated by the arrows. It is seen that the negative bump (a positive charge) appears at the left end of the irradiated area, while the positive bump (a negative charge) appears at the dark node next to the right end of the irradiated area. This asymmetric profile is caused by the one-way electron flow due to the asymmetric bias condition. Potential profiles corresponding to Figs. 4 (a) and (b) are shown in Figs. 5 (a) and (b). It is obvious that photoirradiation produces an almost flat potential in the whole irradiated area, because the charge bumps at the dark/bright boundaries serve to screen the electric field by the bias potential.

In Fig. 4 (b), as mentioned above, the magnitude of the charge fluctuation in the dark area is not much smaller than the charge bumps at the dark/bright boundaries. The magnitude ratio of the bumps at the edges to the fluctuation in the dark area becomes higher for a higher bias voltage (1 V), as shown in Fig. 6, where (a) and (b) again show charge distributions without and with irradiation (5-node irradiation), respectively. Comparing these results in Fig. 6 with those in Fig. 4, the bumps grow more efficiently than the fluctuation in the dark area, resulting a higher bump-to-fluctuation ratio. The charge bumps or the resultant flat potential may be more useful and advantageous than the photocurrent in developing

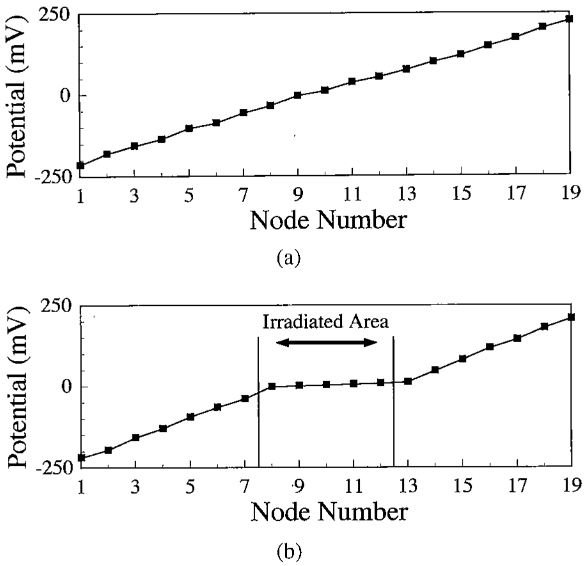

Fig. 5 Potential profiles (a) and (b) corresponding to Fig. 4 (a) and (b), respectively.

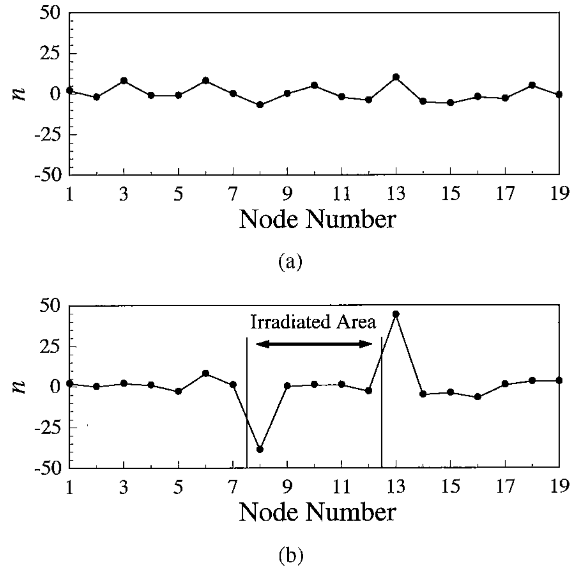

Fig. 6 Charge distributions (number of electrons, *n*, in each node) at $V = 1$ V (a) without irradiation and (b) with continuous irradiation onto 5 middle nodes.

single-electron photonic devices, if their spatial profiles can be successfully measured.

3.3 Irradiation Effects of a Single-Pulse of Light

Next, we have studied a photoresponse of the charge distribution to a single-pulse of light. Figures 7 shows the photoresponse of the charges as a function of time in a number of nodes, (a) to (e), when the bias voltage is 500 mV and 5 middle nodes are irradiated for a period of 100 ps (from $t =$ 100 to 200 ps). In (a) and (e), typical charge fluctuations in the dark area (Node 3 and 16) are shown, which are similar to each other and also similar to those in the other dark nodes.

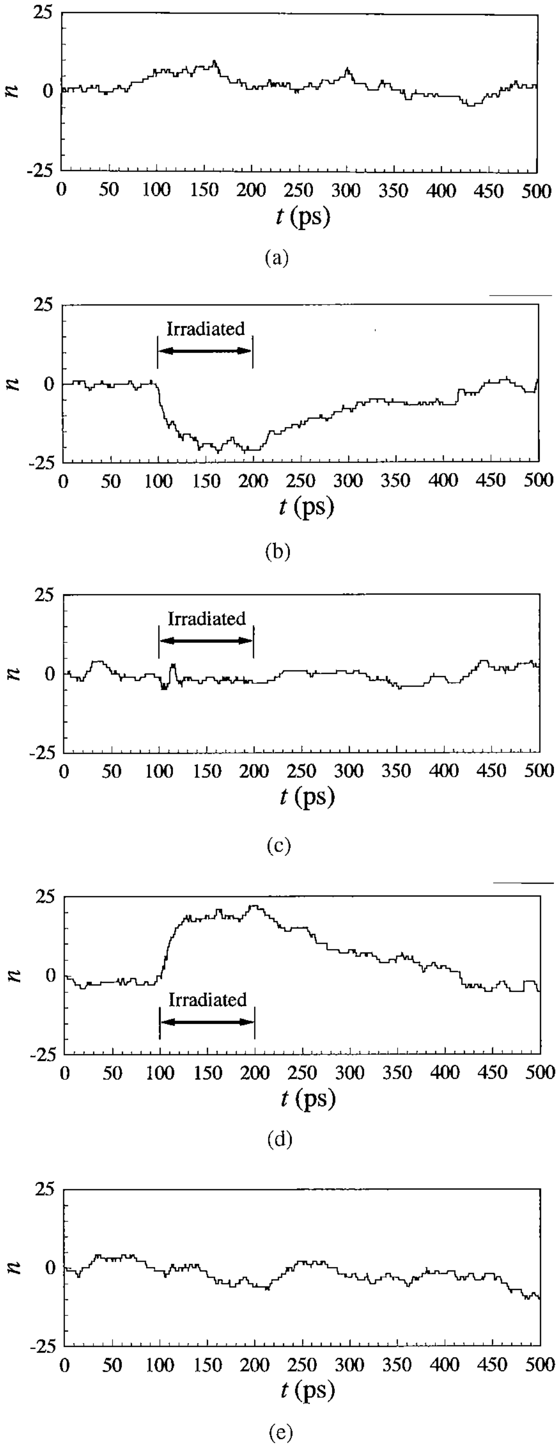

Fig. 7 Photoresponse of charges to a single-pulse of light with a period from $t =$ 100 to 200 ps in (a) Node 3, (b) Node 8, (c) Node 10, (d) Node 13 and (e) Node 16 at $V = 500$ mV. Irradiated area is the middle 5 nodes from Node 8 to Node 12.

In (c), that in the central node (Node 10) with no significant features is shown. In (b) and (d), those in the left edge node of the irradiated area (Node 8) and in the dark node (Node 13) next to the right edge node of the irradiated area are shown. It is found that positive and negative charges start to increase at the onset of irradiation and reach almost constant values with a time constant of about 20 ps. On the other hand, slow decay of the bump charges starts just when the light is shut off with a longer time constant of about 100 ps. The reason of the quick formation of the bumps is that they are formed by SET only through junctions with the small tunnel resistance R_{ph}. On the other hand, the slow decay of the bumps can be accounted for by tunneling through junctions with R_d. In fact, the time constant for the bump formation is close to CR_{ph} (10 ps), while that for the bump decay is close to CR_d (100 ps). This result indicates that the characteristic charge bumps at the dark/bright boundaries would be sustained for a long period, suggesting a photomemory effect, if the dark resistance is satisfactorily high.

3.4 Applicability to Photonic Devices

The results in Figs. 2 and 3 suggest that a SET junction array can be used as photodetectors. So long as the array is not too long (the series resistance in the dark area is not too large), excitation of only a few electrons or even a single electron leads to an appreciable photocurrent. Therefore, it is convinced that the SET junction array has a high sensitivity to excited electrons. For practical application, however, the sensitivity to incoming photons (quantum efficiency) might be more important and the photoabsorption in the volume of the nodes must be taken into account to estimate the sensitivity. The primary advantage in the use of a SET array may be its high spatial resolution limited by the node size typically less than 100 nm, although the resolution is limited also by the photosensitivity.

Another application is suggested by Figs. 4 - 7. If the dark tunnel resistance R_d is satisfactorily high, the specific charge distribution due to irradiation like Figs. 4 (b) and 6 (b) or the potential profile like Fig. 5 (b) will be sustained for a long period after the light is shut off, as manifested in Fig. 7. If we can detect the local potential profile or the local charge distributions, this phenomenon could be applied to photomemory devices with ultra-high resolutions.

4. Conclusion

We have studied photoirradiation effects in a SET junction array by Monte Carlo simulation. The results show generation of photocurrent, of which the magnitude depends on bias voltage and irradiation area. It is also found that under irradiation a characteristic charge distribution (charge bumps at both edges of the irradiated area) is formed, resulting almost flat potential in the irradiated area. Time-response of the charge distribution to a pulse of light is also studied. The decay of the bumps is found to be limited by a time constant, capacitance times tunneling resistance in the dark. Therefore, if the tunneling resistance is high enough, the pulse irradiation can be memorized for a long period. These results suggest feasibility of single-electron photonic devices. Although the model used in this work may be oversimplified, we believe that the present results successfully extract essential points of light irradiation. We have to study further to construct a more practical and precise model including photoabsorption process and modulated electron density of states in the node.

Acknowledgment

This work was partly supported by a Grant-in-Aid for Scientific Research on Priority Area from the Ministry of Education, Science, Sports and Culture.

References

[1] P.K.Tien and J.P.Gordon, "Multiphoton process observed in the interaction of microwave fields with the tunneling between superconductor films," Phys. Rev., vol.129, pp.647-651, 1963.

[2] B.J.Keay, S.J.Allen, Jr., J.Galan, J.P.Kaminski, K.L.Campman, A.C.Gossard, U.Bhattacharya, and M.J.W.Rodwell, "Photon-assisted electric field domains and multiphoton-assisted tunneling in semiconductor superlattices," Phys. Rev. Lett., vol.75, pp.4098-4101, 1995.

[3] P.Delsing, K.K.Likharev, L.S.Kuzmin, and T.Claeson, "Time-correlated single-electron tunneling in one-dimensional arrays of ultrasmall tunnel junctions," Phys. Rev. Lett., vol.63, pp.1861-1864, 1989.

[4] A.N.Cleland, D.Esteve, C.Urbina, and M.H.Devoret, "Very low noise photodetector based on the single electron transistor," Appl. Phys. Lett., vol.61, pp.2820-2822, 1992.

[5] A.Fujiwara, Y.Takahashi, and K.Murase, "Observation of single electron-hole recombination and photon-pumped current in ana asymmetric Si single-electron transistor," Phys. Rev. Lett., vol.78, pp.1532-1535, 1997.

[6] N.Kuwamura, K.Taniguchi, and T.Hamaguchi, "Simulation of single-electron logic circuits," IEICE Trans., vol.J77-C-II, pp.221-228, 1994.

[7] K.K.Likharev, N.S.Bakhvalov, G.S.Kazacha, and S.I.Serdyukova, "Single-electron tunnel junction array: An electrostatic analog of the Josephson transmission line," IEEE Trans. Mag., vol.25, pp.1436-1439, 1989.

[8] M.Tabe, N.Asahi, Y.Amemiya, and Y.Terao, "Simulations of relaxation processes for non-equilibrium electron distributions in two-dimensional tunnel junction arrays," Jpn. J. Appl. Phys., vol.36, pp.4176-4180, 1997.

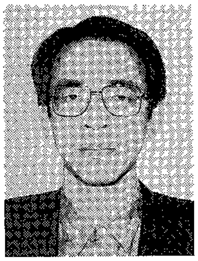

Michiharu Tabe was born in Shiga, Japan, on February 10, 1951. He received the B.S. M.S. and Ph.D degrees from Keio University, in 1973, 1975 and 1984, respectively. From 1975 to 1994, he worked at NTT LSI Laboratories, Atsugi, Japan in a research field of Si epitaxy, ultra-thin gate oxide and Si nano-devices. In 1984 - 85, he worked at Stanford University as a visiting researcher for Si surface studies with Synchrotron radiation. Since 1994, he has been a professor of Research Institute of Electronics, Shizuoka University, Hamamatsu, Japan. He is currently engaged in research on Si-based single electron devices, nanofabrication technologies, self-organization phenomena on the Si surface and their application to photonic devices. Dr. Tabe is a member of the Japan Society of Applied Physics and the Physical Society of Japan.

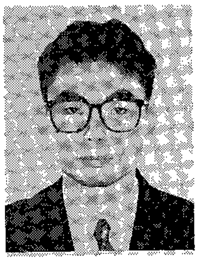

Yoichi Terao was born in Aichi, Japan, on April 7, 1972. He received the B.S. degree from Aichi University of Education, Japan, in 1996. He is currently working toward the M.S. degree in Electrical Engineering at Shizuoka University. His current interests are single-electron tunneling devices and related photonic devices. Mr. Terao is a member of the Japan Society of Applied Physics.

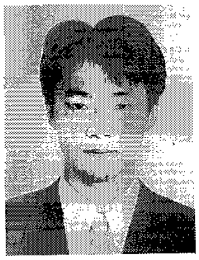

Noboru Asahi was born in Hokkaido, Japan, on July 27, 1971. He received the B.E. and M.E. degrees in electrical engineering from Hokkaido University, Japan, in 1994 and 1996, respectively. He is currently working toward the Ph.D. degree in electrical engineering at Hokkaido University. His current research interests are analog neural LSI's and single electron tunneling devices. Mr. Asahi is a member of the Japan Society of Applied Physics.

Yoshihito Amemiya was born in Tokyo, Japan, on March 5, 1948. He received the B.E., M.E., and Dr.Eng. degrees from the Tokyo Institute of Technology, Tokyo, Japan, in 1970, 1972, and 1975, respectively. From 1975 to 1993, he was a member of the Research Staff at NTT LSI Laboratories, Atsugi, Japan. Since 1993, he has been a professor in the Faculty of Electrical Engineering at Hokkaido University, Sapporo, Japan. His research is in the field of semiconductor materials, devices, LSI design and technology, neural networks, and intelligent material systems and structures. Dr. Amemiya is a member of the Institute of Electrical Engineers of Japan, and the Japan Society of Applied Physics.